Technical Document

PD measurement above 1 MHz (IEC 60270) - limitations, challenges, solutions

P. Mraz, M. Eckert, U. Hammer

TD-118

HAEFELY

Current and voltage – our passion

PD MEASUREMENT ABOVE 1 MHZ - LIMITATIONS, CHALLENGES, SOLUTIONS

Petr Mráz*, Manuel Eckert, Urs Hammer

Haefely AG, Basel, Switzerland
**Email: pmraz@haefely.com*

Keywords: Partial discharge, IEC 60270, frequency range, signal-to-noise ratio, background noise, sensitivity

Abstract

Partial discharge measurement has become a well-accepted and widespread diagnosis method. The IEC 60270 international standard defines how partial discharge should be measured, i.e. how to quantify partial discharge and how to perform the measurement in a plausible, repeatable, and comparable manner. However, recently measurements outside the frequency range recommended by IEC 60270 have become popular. The higher bandwidth approach claims to provide a higher signal-to-noise ratio due to lower background noise levels. This paper revises the IEC 60270 frequency range limitations and analyses measurements above those boundaries. The theoretical hypotheses are then verified by practical measurements. Limitations of such measurements are discussed, especially for large test objects or test objects with windings. The usage of the term "measurement" versus the term "indication" as well as the plausibility, repeatability, and comparability of such partial discharge measurements is discussed.

1 Introduction

Over the past decades, partial discharge (PD) measurement has become one of the most popular diagnostic and quality assurance techniques for high voltage (HV) apparatus. In contrast to other diagnosis methods, PD offers a broader view of the test object condition and provides a hint of interpretation of the fault type. However, PD is one of the most complex methods combining (digital) signal processing, high voltage test techniques, and material science. IEC 60270 [1] has condensed the knowledge from all those fields and defines the basic recommendation and limitations to reach comparable, repeatable, and plausible test results. With the increasing popularity of PD measurements, many alternative so-called non-conventional methods have emerged. Initially, those methods with their indicative nature have been utilized predominantly in the monitoring field. However, recently some of those non-conventional techniques find increasing applications even with ambitions to replace and supplement conventional (electrical) measurements according to IEC 60270. One of those non-conventional test techniques focuses on measurements above the 1 MHz frequency limit of [1]. This trend has become popular, especially with the advent of modern PD detectors enabling measurements up to 20 MHz and beyond. Besides the different measuring frequencies, another differentiation is made regarding the measured quantity – apparent/induced charge [2, 3] versus e.g. the peak voltage amplitude of the PD pulse, various derived quantities, or relative quantities expressed in dB, dBm, etc.

2 Partial discharge theory discussion

The conventional electrical PD test setup according to [1] consists of the voltage power source to energize the test object, an HV filter (i.e. blocking impedance to separate the PD measuring loop from the power supply), the coupling capacitor together with a measuring impedance (AKV) and finally the test object (see Fig. 1). A more detailed description of the test setup and its components can be found for example in [4].

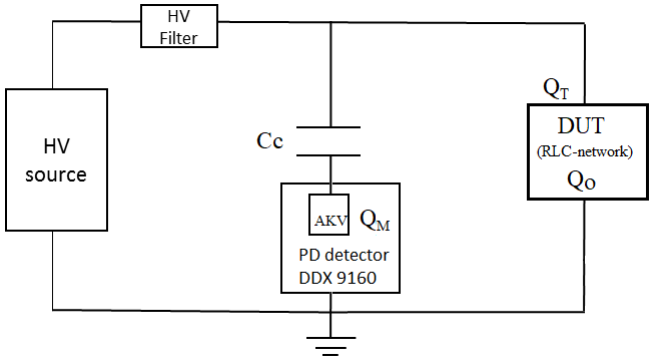

Fig. 1: Conventional electrical PD test setup with a measuring impedance (AKV) integrated inside the PD detector.

The IEC 60270 standard differentiates between wide-band and narrow-band PD measurements. Wide-band measurements have dominated over the past decades because of their robustness, simplicity, and lower probability of error generation. The recommendation for the measuring frequency range is defined by the lower cut-off frequency f_1, the upper cut-off frequency f_2, and the bandwidth (BW) Δf. The lower cut-off f_1 has been defined in the 1960s and is set in the range between 30 – 100 kHz. In the year 2015, the upper cut-off frequency f_2 was increased from 500 kHz to 1 MHz, and the bandwidth Δf was increased from 100 – 400 kHz to 100 – 900 kHz accordingly. However, a very important note has been added which states that for large test objects or test objects including windings, such as transformers or rotating

machines, the upper cut-off frequency f_2 shall remain as low as possible but no more than a couple of hundred kHz. This note is very important and takes into consideration the RLC characteristics of the test objects. For large test objects, the PD frequency content drops drastically due to the loop inductance. Unfortunately, this note is often ignored or misinterpreted. The higher cut-off frequency and BW extension introduced in 2015 as an amendment to [1] aim especially at improving the measurement sensitivity for power cables or single GIS compartments. Due to their coaxial nature power cables and single GIS compartment provide relatively high BW and hence higher sensitivity. In other words, a better signal-to-noise ratio (SNR) can be achieved in case of low noise in the measuring range.

The relationship between the time domain and frequency domain representation of a pulse signal is determined by the fact that shorter pulses in the time domain are characterized by a wider bandwidth in the frequency domain. This is illustrated in Fig. 2 for a PD calibration pulse and an oscillating pulse measured at the terminals of a test object (DUT).

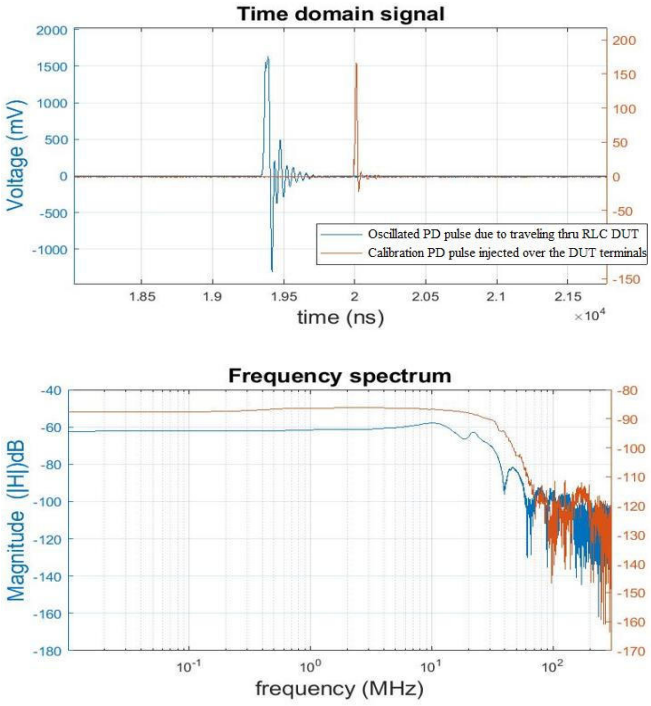

Fig. 2: Time domain (top) and frequency domain (bottom) representation of two PD pulses.

2.1 PD test circuit analysis

Once Looking at the standard IEC 60270 measuring circuit a common misconception is to extract the coupling capacitor (denoted C_k or C_c) from the complete circuit and to claim a high pass (HP) filter behaviour of the reduced circuit with a cut-off frequency f_c defined as

$$f_c = 1/(2\pi RC) \qquad (1)$$

Fig. 3 shows an example of a coupling capacitor of 80 pF and a measuring impedance of 50 Ω. Using Eq. 1 and circuit analysis software results in a 3 dB cut-off frequency of 40 MHz This can lead to the wrong assumption that for this combination of the coupling capacitor and the measuring impedance PD measurements should be conducted above this frequency.

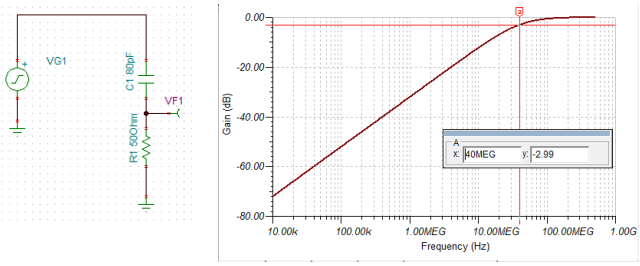

Fig. 3: Frequency analysis of an 80 pF coupling capacitor in series with a 50 Ω measuring impedance.

However, the previous circuit analysis neglects the influence of the test object. Once the test object is added to the circuit and the inductance of the HV connection is taken into consideration the circuit behaves as a low pass (LP) filter with a cut-off frequency of only a couple of MHz. Furthermore, the circuit of Fig. 3 describes a voltage transfer function (U_2/U_1) whereas for PD measurements the circuit transfer impedance (U_2/I_1) must be considered.

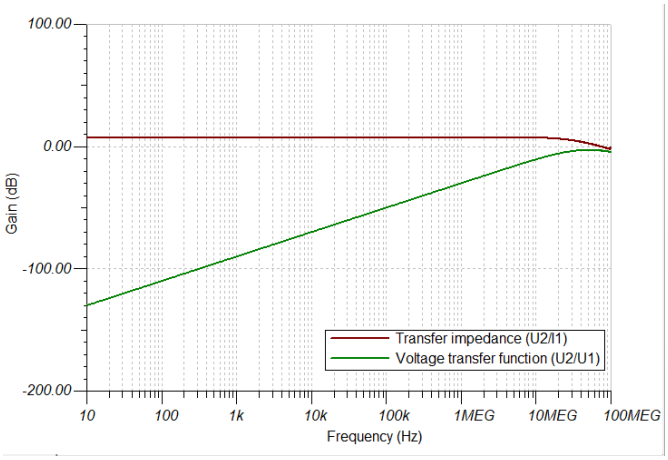

Fig. 4: Frequency analysis of the complete PD circuit, C_c = 100 pF with 50 Ω measuring impedance in series and test object connected in parallel (C_{DUT} = 2 nF).

As shown in Fig. 4 the transfer impedance of the complete PD circuit including the test object (DUT, C_{DUT} = 2 nF) and C_c = 100 pF forms an LP circuit with a -3 dB cut-off frequency at ca. 40 MHz. The higher the capacitance of either C_c or C_{DUT}, the lower the cut-off frequency (C_c = 1 nF ~ 4.8 MHz; 10 nF ~ 1.9 MHz for C_{DUT} = 2 nF). Adding a typical inductance of 1 µH/m for the connection between C_c and the measuring impedance, the cut-off frequency drops to 25 MHz for a connection length of 1 m and 11.5 MHz for a connection length of 5 m, respectively. The lower cut-off frequency remains unaffected.

For verification of the simulations, practical measurements were conducted using a PD setup based on small components with a total loop length of 50 cm. For more accurate modelling of the test setup also the stray inductance of the capacitors must

be considered as shown in the transfer impedance of Fig. 5. It can be concluded that the stray inductances of connection leads and the inherent inductance of the capacitors are the main factors limiting the cut-off frequency.

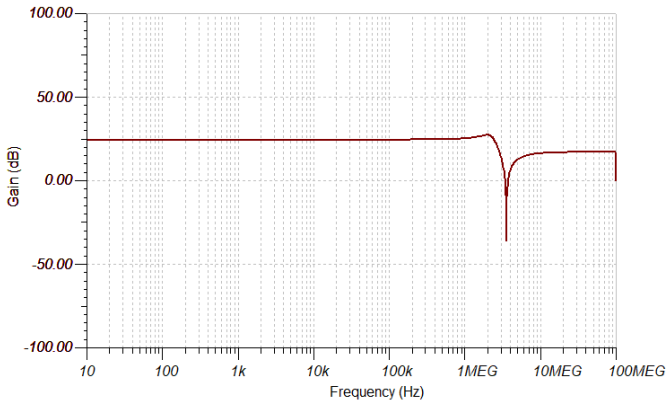

Fig. 5: Transfer impedance of the complete PD circuit with C_c = 1 nF, C_{DUT} = 2 nF, 1 uH in series with the capacitors, and 5 uH between C_c and C_{DUT}.

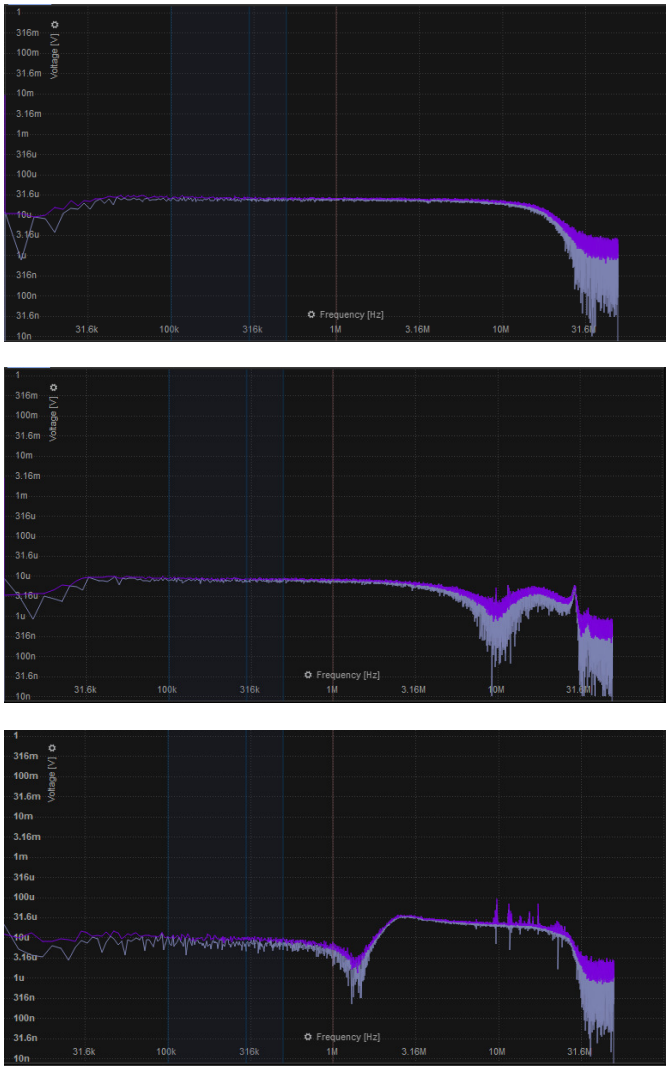

Fig. 6: Frequency spectrum of the 100 pC calibration pulse. Direct PD pulse coupling into the measuring impedance (top); PD calibrator at DUT with a total setup loop length of 50 cm (middle); PD calibrator at DUT with 5 m connection between DUT and a coupling capacitor (bottom).

A Haefely DDX 9160 PD detector with an integrated 50 Ω measuring impedance was used together with a Haefely KAL 9520 PD calibrator [5]. The PD detector allows measurements up to 20 MHz and features an integrated high-resolution spectrum analyser from 0 – 50 MHz with a resolution of 2.5 kHz. In Fig. 6 it can be clearly seen that the loop size (and its inherent inductance) reduces the BW of the calibration pulse from 20 MHz down to 1 MHz only.

Madhar et al. [4] have demonstrated that already the high voltage coupling capacitor itself limits the BW of the measurement due to the inherent inductance depending on the size of the coupling capacitor (see Fig. 7). It can be concluded that for frequencies above 1 to 1.5 MHz, the electrical characteristics of the coupling capacitors becomes inductive. Therefore, PD measurements cannot be performed in frequency intervals containing resonance frequencies due to an undefined/unstable transfer impedance which renders the charge calibration invalid.

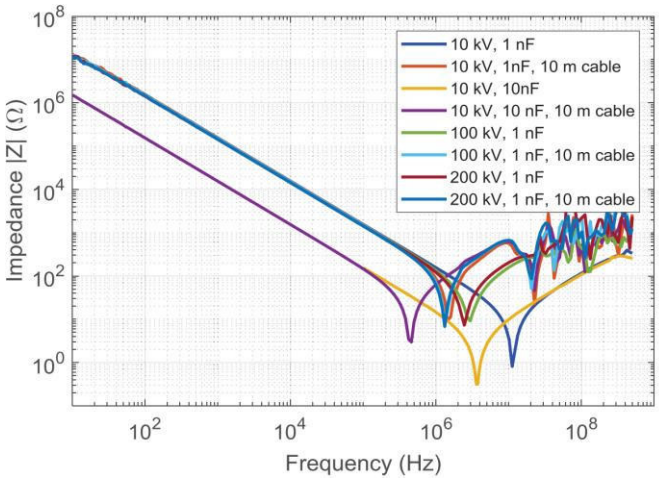

Fig. 7: Impedance of capacitors with various capacitance values, physical size, and measuring loop lengths [4].

2.1 Charge integration principle

The IEC 60270 standard uses either the term apparent charge, induced charge, or simply charge Q expressed in Coulombs (typically pC or nC). This charge is an integrated value of the high-frequency current which represents the PD events. The benefit of the signal integration in comparison with e.g. a peak voltage measurement is the property that even though the PD pulse changes its shape (it is attenuated or oscillating because of travelling thru the DUT) the area underneath the pulse current curve remains constant, i.e. the integrated charge value is independent of the peak voltage/current value.
However, this principle of charge quasi-integration needs to fulfil one important criterion. The integrated calibration pulse (for a given measuring frequency range) must look the same as the real (measured) PD pulse. which is of course difficult to verify in the time domain. Hence, it is recommended to apply a frequency domain pulse analysis, where the measuring frequency shall be selected within the flat part of the pulse

spectrum, avoiding any resonance peaks, significant signal drops, or decays.

A step-by-step guideline for PD measurements is outlined in [6] as follows:

- Step 1: Checking the noise spectrum
- Step 2: Checking the calibration spectrum
- Step 3: Analysing the real PD pulse spectrum

The importance of this step-by-step guideline and its influence on the plausibility, repeatability, and comparability of the results is demonstrated in the following section.

3 Results

Two stator coils have been selected as test objects. The first one is a relatively small coil of a 6.6 kV, 700 kW motor with a total coil loop length of 2 m (end-to-end). The second coil is from an 11 kV, 32 kVA generator with a total coil loop length of 7.5 m. A stator coil has a different characteristic to the stator bar which can be modelled as a transmission line that goes in series with an inductance (end-winding part). The stator coil consists of the stator part and end-winding parts at the same time and accommodates multiple turns. Hence, its frequency characteristics exhibit multiple resonant points like a transformer coil where L and C combinations must be considered as shown in Fig. 8. Further details can be found e.g. in [7]. The 6.6 kV coil has 3 turns – please refer to Fig.8, Fig. 9, and Fig. 10 and note the corresponding resonances.

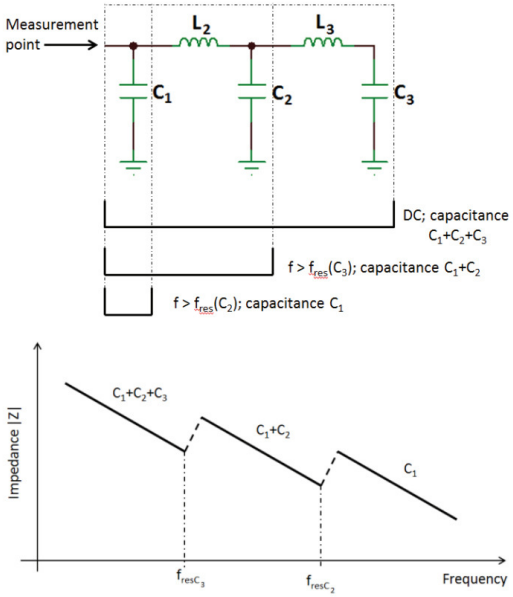

Fig. 8: Simplified equivalent LC circuit (top) and corresponding qualitative frequency response (bottom) of e.g. a stator coil or transformer winding [7].

To confirm the model behaviour described above a Keysight E4990A Impedance Analyzer, (20 Hz to 10 MHz) and a Keysight E5061B Vector Network Analyzer were used to analyse the 6.6 kV stator coil.

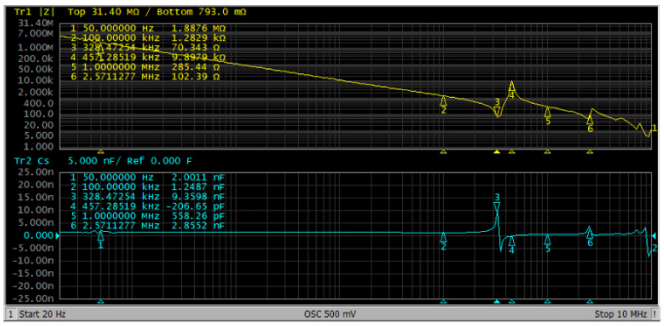

Fig. 9: Transfer impedance Z(f) (top) and capacitance curve C(f) (bottom) of the 6.6 kV stator coil.

Fig. 9 confirms good agreement with the theoretical assumptions previously made. It can be seen that the first resonance appears at ca. 330 kHz (a second resonance at ca. 2.5 MHz), beyond this frequency, a part of the coil capacitance is hidden, i.e. when measuring above 330 kHz only a certain part of the coil is measured/analysed. A significant drop of capacitance from ca. 2 nF to ca. 0.56 nF is observed after the first resonance which indicates that only one-fourth of the coil is effectively analysed when measuring above 330 kHz. In other words, only the part of the coil which is close to the coupling capacitor is considered. At the same time, the capacitance (and hence the PD sensitivity) is increased at the resonance points. However, those values are irrelevant and can be misleading for PD measurements as stated above.

Using an impedance or network analyser might be cumbersome and impractical for on-site testing, besides the fact that the equipment is rather expensive. However, modern PD detectors should be equipped with an integrated spectrum analyser providing the same information. Fig 10 shows an automatic high-resolution fast frequency transform (FFT) analysis up to 50 MHz of the calibration pulse on the 6.6 kV stator coil indicating good agreement with the measurement shown in Fig. 9.

Table 1 shows the difference in the PD values when calibrated at the "near-end" (terminal connected to the coupling capacitor) versus the "far-end". The root cause of the difference is directly visible when looking at the FFT spectrum of the calibration pulse (Fig. 10) – the signal gain, respectively loss of signal caused by the resonance at 330 kHz. This behaviour can be confirmed using a simple LC network and a circuit simulator as illustrated in Fig. 8.

Table 1 Near-end versus far-end calibration using a 100 pC calibration pulse, where near-end calibration was considered as the reference.

Calibrator @	30 – 130 kHz	100 – 500 kHz
Near-end	102 pC	99 pC
Far-end	111 pC	228 pC

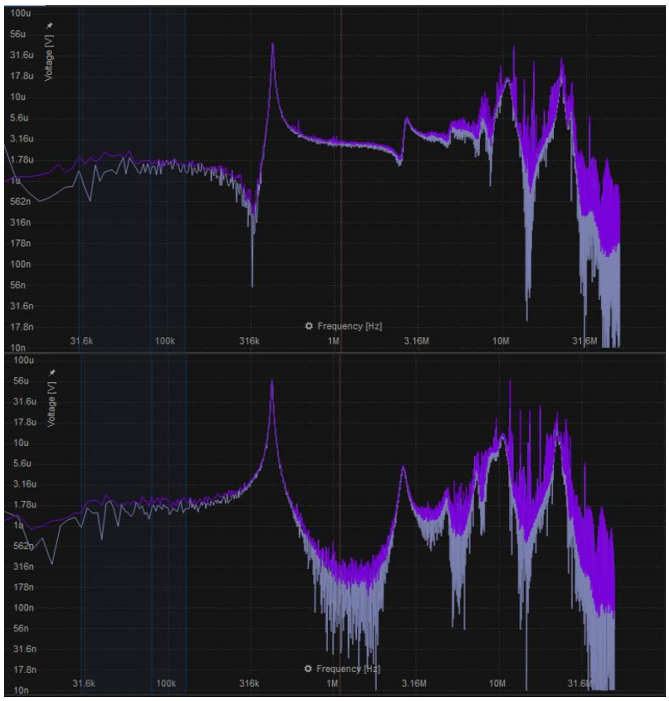

Fig. 10: FFT of the PD calibration pulse at the near end (top) and far end (bottom) of the 6.6 kV stator coil.

The same behaviour could also be observed when using a C_c value of 0.1, 1, or 10 nF. The difference was the signal sensitivity where the difference in the SNR between 0.1 nF and 10 nF was a factor of 15, i.e. when using a 10 nF coupling capacitor PD pulses of 15x smaller amplitude can be measured in comparison to a 0.1 nF coupling capacitor.

To perform measurements up to 20 MHz an EMC-shielded enclosure is required. See the comparison of the frequency spectra in Fig. 10 (outside the shielded room) and Fig. 11 (inside the shielded room) above ca. 10 MHz

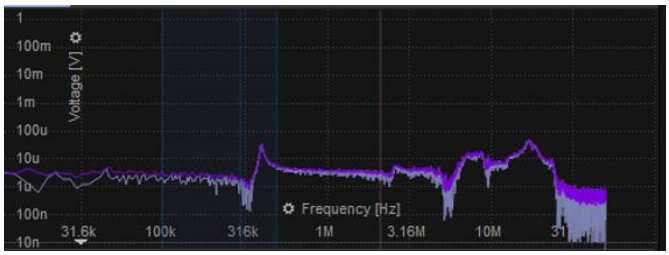

Fig. 11: FFT of the PD calibration at 6.6 kV stator coil.

Looking at the FFT spectrum in Fig. 11 one might assume that a better SNR could be achieved when measuring at higher frequencies (as the signal gain is higher). As per the explanation above, this virtual signal gain is caused by a de-facto cancellation of the capacitance because of the LC resonances. However, the PD detector has been calibrated at five different frequency ranges shown in Table 2 and the PD activity was measured at those frequencies to demonstrate another important phenomenon. The coupling capacitor used was 1 nF to get a reasonable SNR –while using e.g. only 100 pF resulted in too low an SNR. A calibration factor of one represents the direct coupling between the PD detector and the calibrator; a calibration factor of two means that the signal needs to be amplified by a factor of two in comparison to the direct coupling.

Table 2 PD calibration of the 6.6 kV stator coil.

Frequency Range (kHz)	Cal. Factor	PD Source 1 @ 4.2 kV	PD Source 1+2 @ 5.4 kV
100 – 280	14.566	40 pC	10.5 nC
100 – 500	8.397	17 pC	5.36 nC
500 – 2 000	8.494	7. 5 pC	6.31 nC
3 000 – 4 000	6.491	19.7 pC	4.94 nC
7 000 – 8 800	1.804	2.37 pC	0.28 nC
16 500 – 18 000	0.552	0.08 pC	0.014 nC

Table 2 shows that for the 16.5 – 18 MHz frequency range (hitting the resonance with the highest peak) the SNR is very good and the signal gain in comparison to the lowest frequency range is almost a factor of 30. However, the real PD shows exactly the opposite behaviour. The FFT plots of Fig. 12 and Fig. 13 show that the real PD signal has barely any content above ca. 4 MHz In the case of «PD Source 1», very poor and unclear PD activity could be recognized in the phase-resolved PD (PRPD) pattern, and no PD activity could be recorded above 7 MHz In the case of «PD Source 2», the PD activity could be recorded with a disturbed PRPD pattern up to 18 MHz, however, with clear visibility that part of the PD signal (in the mean of amplitude but also pulse repetition rate) is completely lost and the remaining signal is heavily attenuated (a factor of 750 in comparison to lower frequencies). First, because of the nature of the PD failure (each PD defect has a different frequency content) and second because of the different propagation paths (RLC-network, resonances, and signal loss).

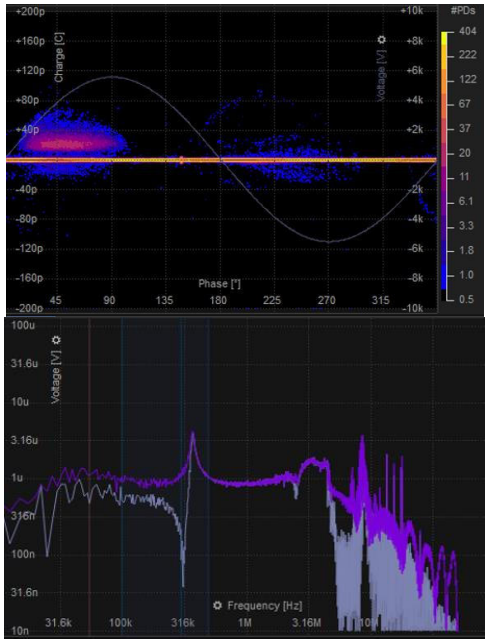

Fig. 12: 6.6 kV stator coil, PD Source 1 @ 4.2 kV, PRPD pattern @ 100 – 280 kHz (top), FFT spectrum of the PD pulse (bottom).

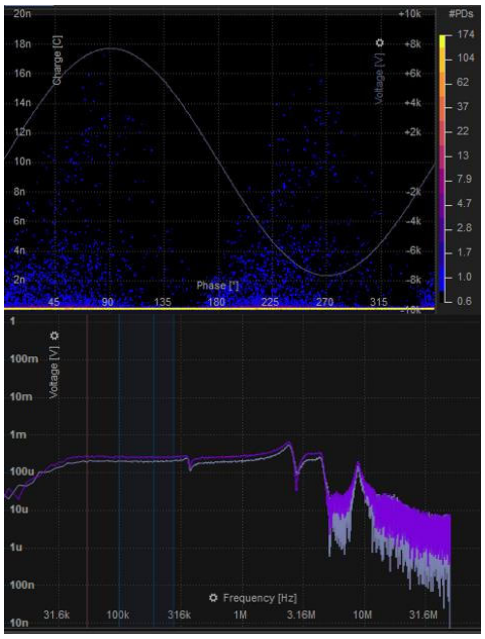

Fig. 13: 6.6 kV stator coil, PD Source 1+2 @ 5.4 kV, PRPD pattern @ 100 – 280 kHz (top), FFT of the PD pulse (bottom).

The same behaviour could be reproduced with the 11 kV stator coil where no PD could be recorded above 5 MHz and already above 2 MHz it was virtually impossible to recognize. For larger PD activity in the nC range the difference between the 100 – 500 kHz and 10 – 20 MHz frequency range was a factor of 20. In addition, the measurement of a complete stator of a 6 kV, 600 kW motor was conducted. The frequency range of 100 – 600 kHz showed a PD value of Q_{iec} = 5 nC but the 100 – 250 kHz range already showed a value of Q_{iec} = 10 nC which brings the status evaluation of the machine from "green/orange" to class "orange/red". Signal attenuation was clearly visible in the FFT spectrum and hence the measuring frequency range has been re-adjusted.

4 Discussion

Provided that the measuring frequency range is properly selected (avoiding any resonances and staying in the flat part of the FFT response) the charge value Q_O at the PD origin (see Fig. 1) is correctly transferred to the DUT terminals (Q_T). This is valid both for lumped (small) capacitive test objects which also have their inherent RLC characteristics (see Fig. 7 and Fig. 8 and reference [7]) and for test objects with windings, large DUTs and test objects with transmission line behaviour (power cables or single GIS compartments) as demonstrated in section 3. The network behaviour of a particular test object can be easily verified using an impedance analyser (Fig. 9) or a frequency response analyser (FRA) [7]. Lemke [2, 3] has proposed the term "induced" rather than "apparent" charge to emphasize the direct relation between the charge at the PD origin Q_O and the charge at the DUT terminals Q_T (see Fig 1). Charge transfer between the DUT terminals and the coupling capacitor is ensured by the PD calibration process. The ratio between the charge Q_T and the so-called measured charge Q_M at the measuring impedance (see Fig. 1) is a measure of the sensitivity of the measuring circuit with the general rule that an increase of the total capacitive load will lead to a reduced SNR of the measurement.

5 Conclusion

The importance of checking the frequency domain of the PD measurement and proper settings of the measuring frequency range has been demonstrated. IEC 60270 highlights that for large test objects and test objects with windings the upper cut-off frequency f_2 shall be kept as low as possible because of signal attenuation in the higher frequency content of the PD pulse. PD measurement at higher frequencies is possible, but the quantification becomes difficult. PD sources located further from the coupling capacitor tend to be omitted and the overall measurement plausibility becomes questionable. The term «PD indication» (rather than PD measurement) shall be used for such measurements. We have demonstrated that electrical PD measurement quantified by the charge value within the frame of IEC 60270 is the preferred way to conduct plausible, repeatable, and comparable PD measurements with the possibility of a reasonable quantification of the PD failure level. The frequency characteristics of the complete PD test setup (valid not only for RLC test objects) should be kept in mind, especially when comparing different PD detectors.

6 References

[1] IEC 60270:2000+AMD1:2015: "High-voltage test techniques - Partial discharge measurements", Ed. 3.1, 2015.
[2] E. Lemke, "A critical review of partial-discharge models" IEEE Electrical Insulation Magazine, vol. 28, no. 6, pp. 11-16, Nov-Dec 2012.
[3] E. Lemke, "Analysis of the partial discharge charge transfer in extruded power cables" IEEE Electrical Insulation Magazine, vol. 29, no. 1, pp. 24-28, Jan-Feb 2013.
[4] S. Abdul Madhar, et al, "Frequency Response of a Real Cable Network and its Impact on Field PD Measurements", 25th International Conference on Electricity Distribution, Madrid, Spain, June 2019.
[5] Haefely AG, "DDX 9160 / 9161 Partial Discharge Detector", Operating Manual, V1.0.
[6] P. Mraz, S. A. Madhar, P. Treyer, U. Hammer, "Guidelines for PD measurement according to IEC 60270", In ISH 2019: Proceedings: 21st International Symposium on High Voltage Engineering, Budapest, Hungary, 2019.
[7] P. Mraz, P. Treyer, U. Hammer, S. Gonzalez, "Innovative Application of Frequency Response Analysis for Partial Discharge Measurement". In ISH 2015: Proceedings: 19th International Symposium on High Voltage Engineering, Pilsen, Czech Republic, 2015.

Designed by

Tettex INSTRUMENTS

Global Presence

EUROPE
HAEFELY AG
Birsstrasse 300
4052 Basel
Switzerland

☎ + 41 61 373 4111
☞ sales@haefely.com

CHINA
HAEFELY AG Representative Office
8-1-602, Fortune Street, No. 67
Chaoyang Road, Beijing 100025
China

☎ + 86 10 8578 8099
☞ sales@haefely.com.cn

INDIA
HAEFELY India Service Office
C/o Pfiffner Instrument Transformers Pvt. Ltd.
176, 178/2 Sarul, Viholi
Nashik 422 010, India.

☎ +1 800 266 4052 (toll free)
☞ sales@haefely.com

The original version of this article was published in the 23rd International Symposium on High Voltage Engineering, Glasgow, Scotland, UK, 2023.

This is the author's pre-print edition.

HAEFELY
Current and voltage – our passion

HV HIGH VOLTAGE
I INSTRUMENTS
E EMC

precision. swiss made.